METEORS AND ATMOSPHERES

W.J. Baggaley
Physics Department, University of Canterbury, Christchurch,
New Zealand.

ABSTRACT

Meteoroid ablation in an atmosphere produces a weak plasma column. The processes important in governing the state of the meteoric species subsequent to column formation are reviewed. The actions of transport and of chemical reactions in controlling the life of the various species in the column are described. It is found that the interaction of meteoric ions with atmospheric gases leads to the dissipation of ionization and is the source of anomalous radio-meteor echo characteristics: recognition of these effects is important in permitting meaningful interpretations of radio-meteor data. Several modes of interaction between meteoric species and an atmosphere can yield enduring emissions. The fate of the various species is discussed.

1. INTRODUCTION

The purpose of this review is to examine the processes governing the fate of meteoric constituents in, primarily, the earth's atmosphere. The products of meteoroid interaction with atmospheric gases are subject to various dynamical, physical and chemical processes which lead to their dispersal and eventual fall-out or rain-out at the earth's surface.

2. ABLATION PRODUCTS

Meteoroids of mass $10^{-8} \lesssim m \lesssim 10^2$ g (representing a large proportion of the particle population mass) having geocentric velocities $11 \lesssim v \lesssim 72$ km s^{-1} (representing particles in closed orbits) ablate where the atmospheric density is in the range 10^{-4} to 10^{-7} kg m^{-3}. For the earth the corresponding heights are between about 70 and 110 km. At these heights the major atmospheric molecules N_2, O_2 and CO_2 maintain approximately the ground level mixing ratios while the concentrations of the minor species O, O_3 and H_2O are governed by photochemical and dynamical processes. Ablation releases meteoric atoms, M, from the

85

meteoroid surface which in several hundred electron-volt impact energy
collisions with atmospheric molecules yield predominantly excited
atoms and ions:

$$M + O_2 \rightarrow M^* + O_2$$

$$\rightarrow M^+ + e + O_2$$
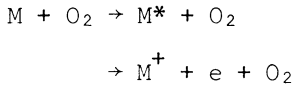
Such processes are known from laboratory studies to dominate over dis-
sociative excitation, dissociative ionization and the excitation of
atmospheric molecules. Momentum loss cross-sections and ionization
cross-sections for these processes are known so that a reasonable
estimate can be made of the yield of ions and neutral atoms. For
simplicity and ignoring such processes as sputtering and the release
of meteoric molecules at low meteoroid velocities, a working model of
ablation products can be established from the cross-sections of Sida
(1969) and with a knowledge of the abundances for stoney meteoroids,
Mason (1971) (Table I). The probability β, that a meteoric atom will produce an electron in its thermalizing collisions depends on meteoroid velocity but is more strongly velocity dependent for oxygen atoms (O) than for metals (M); $\beta_o \sim v^5$, $\beta_M \sim v^3$. Table I, ($\beta = 0.031$ for $v = 40$ km s^{-1}) covering the most abundant meteor species represents a convenient working model and can form the basis for a discussion of the subsequent behaviour of a meteoric plasma.

Table I.

	atom %	ion
O	54.80	2.450
Si	16.60	0.209
Mg	15.65	0.064
Fe	11.37	0.298
Ca	0.87	0.023
Na	0.71	0.045
	100.00	3.089

3. THERMAL HISTORY

Since ablated atoms possess energies > 100 eV the collisional
processes degrade this translational energy into heating of the atmosphere.
Additionally, electrons produced by impact ionization may be expected to
possess a few eV of translational energy. The subsequent electron
energy distribution will be determined by complex collision processes
with electron-electron Coulomb collisions producing a Maxwellian distri-
bution.

Cooling of the neutral gases in the meteor column may be considered
in two stages; a rapid initial adiabatic expansion in which pressure
equalization is achieved with the ambient atmosphere, followed by cooling
by thermal conduction. Since both the initial temperature of the column
T_o

$$T_o \; \alpha \; v^2/r_i^2$$

(r_i initial radius) and also the cooling rate increase with increasing height, the time to achieve thermalization is not strongly height dependent. At 95 km and for a magnitude +5 meteor the times to cool to 10 per cent above the temperature of the ambient atmosphere are approximately 0.16, .045 and 0.017s for meteoroid velocities of 30, 40 and 50 km s^{-1} respectively.

Electrons at temperature T_e will cool by encounters with various gas species at temperature T_g and also by thermal conduction (Baggaley and Webb 1977)

$$\frac{dT_e}{dt} = - \frac{2}{3k} \sum C_j(T_e,T_g)n_j + \frac{2}{3k} \nabla \cdot (K_e \nabla T).$$

The second term on the right hand side represents the divergence of the heat flux, where K_e is the electron thermal conductivity and the first term represents encounters with coolant gas of number density n_j, where k is Boltzmann's constant. The collision term C_j is composed of (i) elastic scattering with neutrals, (ii) inelastic scattering with neutrals yielding N_2(vib, rot) and O_2(vib, rot) (iii) elastic scattering with positive meteoric ions (iv) excitation of the fine structure ground state excitation of atomic oxygen ($O(^3P)$). The electron thermalization times (time until $T_e/T_g = 1.1$) for small meteors ($\alpha_e \lesssim 10^{12}$ cm^{-1}) increase from about 10^{-3} s at 80 km to 10^{-1} s at 110 km. For $\alpha_e \gtrsim 10^{12}$ cm^{-1} the cooling is more rapid because of the contribution of positive ion Coulomb scattering.

4. TRANSPORT

Meteoroid ablation deposits meteoric atoms and ions in a column of length many kilometres and diameter $\sim$ 1m so that concentration gradients transverse to the column axis are much greater than those parallel to the axis. Radial expansion of the meteoric atoms is governed by free molecular diffusion, (coefficient D_M) while the ion and electron transport will be governed by ambipolar diffusion (coefficient D_a). When, however, the column diameter becomes comparable to the scale size L of the smallest eddies in the ambient atmosphere, subsequent expansion is governed by turbulent diffusion (coefficient D_e). Solution of the continuity equation

$$\frac{\partial n}{\partial t} = \nabla \cdot (\text{flux}) = \nabla \cdot (D\nabla n) = D\nabla^2 n$$

with n the species number density and ∇^2 the Laplacian in cylindrical coordinates, shows that the Gaussian radius of the column after diffusing for time t from an initial radius r_i is given by $r^2 = r_i^2 + 4Dt$. For a height of 95 km for example $D_a \simeq 3m^2$ s^{-1}, $D_M \simeq 1$ m^2 s^{-1}, $D_e \simeq 200$ m^2 s^{-1} so that turbulent diffusion will lead to rapid dispersal after about 75 s while disruption of the column by non linear winds will occur within a few seconds of formation.

5.   THE INTERACTION OF METEORIC POSITIVE IONS WITH THE ATMOSPHERE

Gas phase reactions between various species of ions, atoms and molecules of atmospheric interest have been the subject of laboratory measurements and atmospheric - ionospheric studies for several years. In consequence it is now possible to develop useful models of the interaction of meteoric species with the atmosphere. Rate coefficients for reactions between meteoric species and atmospheric constituents are temperature dependent. However in the following sections rate coefficients (k, cm^3 s^{-1}) appropriate to 200 K will be employed (unless otherwise stated) to calculate instantaneous time-constants, τ, thus permitting estimates of the lifetimes of various species. Since sources of the appropriate reaction rate coefficients and of atmospheric constituent number densities are available in several reviews (e.g. Brown 1973, CIRA 1972), they are not referenced in detail here. As a working model we shall assume that a 1 g 40 km s^{-1} meteoroid deposits a peak ionization density of $\alpha_e = 10^{14} cm^{-1}$ at a height of 95 km.

5.1   The fate of metal ions

Since the ionization potentials of metal atoms IP(M) are 5-9 eV and less than those of O_2 and N_2, M^+ ions are stable against charge exchange with major neutrals. Because M^+ - electron radiative recombination is very slow while three body recombination will not be of importance at heights > 80 km, the process most active in destroying metal ions is oxidation in the presence of ozone

$$M^+ + O_3 \rightarrow MO^+ + O_2 \qquad\qquad k \simeq 2 \times 10^{-10}$$

yielding $\tau \sim 50$ s at 95 km. For low plasma density meteor columns, reduction with atomic oxygen

$$MO^+ + O \rightarrow M^+ + O_2 \qquad\qquad k \sim 10^{-10}$$

with $\tau \sim 0.1$ s at 95 km will dominate while with a dense plasma dissociative recombination will be more important

$$MO^+ + e \rightarrow M + O \qquad\qquad k \sim 10^{-7}$$

yielding, with $\alpha_e = 10^{14} cm^{-1}$ and $r_i = 1$ m, $\tau \simeq 3 \times 10^{-3}$ s. At lower heights (h < 80 km) three body oxidation may be expected to produce MO_2^+ and MN_2^+ ions where for large meteors dissociative recombination will occur faster than either reduction or collisional break-up. The coupled set of diffusion equations including the appropriate chemistry can be solved (Baggaley 1978a) giving the life history of the various species.

An important observational consequence is the destruction of electrons in the expanding meteor train. A radar echo from a column of meteoric ionization will endure as long as the electron concentration near the column axis is above the critical density for the radio

wavelength employed (overdense echo). There exist three types of observational data confirming the ionization depletion models outlined above.

(i) Multistation radar observations of rough (i.e. no longer specular scattering operative) trains (McKinley 1956) gave the height dependence of the ionization loss showing a rapid depletion below ~ 90 km (Baggaley 1978a).

(ii) Observations of a large number of overdense-type echoes show that the most probable height of an echo is ~ 93 km (McKinley 1961).

(iii) The number versus overdense echo duration characteristics shows a depletion of echo numbers for durations in excess of about 10 s. In particular these characteristics show a diurnal variation with more long enduring echoes being recorded during daytime. This "sunrise effect" has been reported by Hughes and Baggaley (1972) and Nicholson and Poole (1974) for Quadrantid meteors and by McIntosh and Hadjuk (1977) for sporadic meteors.

A comparison of the observations with theory indicates that ionization depletion is controlled by ambipolar diffusion above 93 km and by chemical destruction below 93 km.

5.2 The fate of atomic oxygen ions

O^+ ions behave quite differently to M^+ ions: since $IP(O) > IP(O_2, N_2)$ charge exchange with major atmospheric neutrals can occur;

$$O^+ + O_2 \rightarrow O_2^+ + O \qquad\qquad k = 2.5 \times 10^{-11}$$

$$O^+ + N_2 \rightarrow NO^+ + N \qquad\qquad k = 2.0 \times 10^{-12}$$

so that $\tau_{O^+} \sim 10^{-2}$ s at 95 km. Ground state O_2^+ ions react very slowly by atom-atom interchange with N_2 or with trace constituents NO and N while NO^+ reacts only by three-body association with the major atmospheric gases. The dominant loss process for the diatomic ions will be by dissociative recombination

$$O_2^+ + e \rightarrow O + O \qquad\qquad k = 2.2 \times 10^{-7}$$

$$NO^+ + e \rightarrow N + O \qquad\qquad k = 7.0 \times 10^{-7}$$

with $\tau_{O_2^+} \sim 3 \times 10^{-3}$ s and 0.3 s for meteors of approximate magnitudes 0 and +5 respectively. The set of coupled diffusion equations can be solved to calculate the loss of electrons in the diffusing plasma. This has been done in Baggaley (1979a) for the case of underdense meteor plasma at heights > 95 km: recombination effects are shown to be insignificant for radar observation employing frequencies $\gtrsim 20$ MHz. However, for long wavelength observations or for meteors at heights $\lesssim 85$ km, electron loss time-constants due to O^+ disappearance can be comparable with the echo decay time-constant

$$\tau_d = \lambda^2 / 16\pi^2 D_a$$

of an underdense echo. Observational evidence for a significant ioniz-
ation loss comes from measurements of the decay constants of underdense
echoes.

(i) Brown (1976) measured the height variation of decay constants
using the low radio frequency of 1.98 MHz. The author reported that
- "below a height of 105 km the decay times level off and are scattered
about a value of approximately 4s". Since at 100 km $\tau_d \sim$ 10s for 1.98
MHz reference to Baggaley (1979a) shows that indeed an O^+-e lifetime
of $\sim$ 4s is to be expected at 100 km.

(ii) Measurements of the height variation of the apparent diffusion
coefficient, D_a, by Baggaley and Webb (unpublished) show that for heights
$\lesssim$ 85 km values of measured D_a are greater than the values expected from
the known scale height.

6. REACTION ENERGY CHANNELLED INTO LIGHT

The collisional excitation of neutral meteoric atoms and ions result-
ing from thermalizing impacts during plasma column formation yields the
impact (primary) radiation of a meteor. However, the creation energy of
metal ions (5-9 eV) and oxygen ions (13.6 eV) originating in collisional
ionization is well in excess of that corresponding to visible radiation
and it is of interest to enquire whether this energy can be channelled
into atomic and molecular transitions to yield an enduring luminosity.
Naked eye observations of meteor train emission enduring for (rarely) up
to an hour have been reported while trains of duration $\sim$ 1 s are a feature
of high velocity meteor showers (e.g. Perseids, Orionids, Leonids).
Unfortunately spectral information on long enduring trains is entirely
lacking.

6.1 Metal ions

The process of dissociative recombination of metal oxide ions
(section 5.1) has an exothermicity

$$\Delta H = IP(MO) - D_o(MO)$$

and Table I gives the low-lying spin-allowed product atomic states that
are possible in the dissociation process. The multiplet nomenclature is
that of Moore (1972) and uncertainties in ΔH arise from uncertainties
in oxide dissociation energies. The calculation by quantum mechanical
methods of the rate coefficients for dissociation into specific states
is not possible for many-electron systems. However recourse can be made
to a statistical approach involving the total number of repulsive MO
states that correlate with specific product atomic states. Such a
treatment has been carried out by Poole (1979) to estimate the strengths
of transitions to be expected as a result of recombination. The emission
per unit length of train is governed by the slow formation of MO^+ and the
temporal characteristics expected from the processes were found by Poole
(1978) to be compatible with Baker-Super-Schmidt camera records of two
persistent trains obtained in 1953-4 during the Harvard Meteor Project.

Table II: Transitions expected from dissociative recombination.

	ΔH eV	state	excitation energy eV	transition	wavelength Å
Fe	4.5 ± 0.2	$z^7D°$	2.48	$a^5D - z^7D°$	5110(1)
		$z^7F°$	2.88	$- z^7F°$	4427(2)
		$z^7P°$	3.03	$- z^7P°$	4216(3)
		$z^5D°$	3.29	$- z^5D°$	3860(4)
		$z^5F°$	3.42	$- z^5F°$	3720(5)
Mg	5.0 ± 1	$^3P°$	2.70	$^1S - {}^3P°$	4571(1)
		^3S	5.09	$^3P - {}^3S$	5183(2)
Si	4.0 ± 0.3	$^3P°$	4.91	$-$	$-$
Ca	2.6 ± 1	$^3P°$	1.88	$^1S - {}^3P°$	6572(1)
		$^1P°$	2.93	$^1S - {}^1P°$	4226(2)
Na	4.7 ± 0.5	$^2P°$	2.09	$^2S - {}^2P°$	5896(1)

6.2 Oxygen ions

Consider now the energy available from the formation of O^+ ions (13.6 eV) and the energetics of the reactions introduced in section (5.2). Charge exchange processes

$$O^+(^4S) + O_2(X^3\Sigma_g^-) \rightarrow O^+(^2\pi_g) + O(^3P) + 1.55 \text{ eV}$$

$$+ N_2(X^1\Sigma_g^+) \rightarrow NO^+(^1\Sigma) + N(^4S) + 1.10 \text{ eV}$$
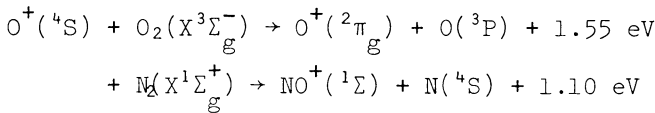
lead to subsequent dissociative recombination for which laboratory measurements are available giving the branching ratios into specific product states (Sharpe et al. 1975; Kley et al. 1977)

$$O_2^+(^2\pi_g) + e \rightarrow O + O \quad \Delta H = IP(O_2) - D_o(O_2) = 7 \text{ eV}$$

$$NO^+(^1\Sigma) + e \rightarrow O + N \quad \Delta H = IP(NO) - D_o(NO) = 3 \text{ eV}$$
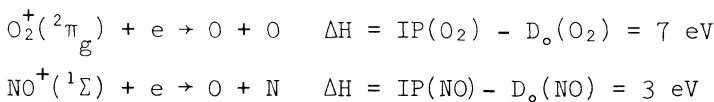
Possible states are $O(^3P, {}^1D, {}^1S)$ and $N(^4S, {}^2D)$, $O(^3P)$. The possible excited states of O and N are all metastable so that collisional de-activation may be an important process:

$$O(^1D) + O_2 \rightarrow O(^3P) + O_2^* \quad k = 6 \times 10^{-11}$$

$$+ N_2 \rightarrow O(^3P) + N_2^* \quad k = 5 \times 10^{-11}$$

$$N(^2D) + O_2 \rightarrow NO + O \quad k = 6 \times 10^{-12}$$
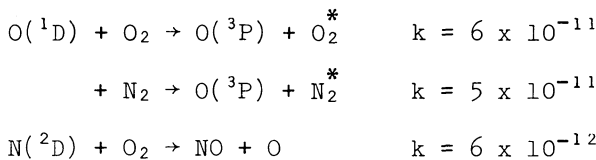
provide deactivation rates for $O(^1D)$ of $4 \times 10^3 s^{-1}$ and $10^2 s^{-1}$ at 90 and 110 km respectively and for $N(^2D)$ $4 \times 10^2 s^{-1}$ and $10 s^{-1}$. Consider the case of the red 6300 Å doublet transition. The volume emission rate is equal to the product of the $O(^1D)$ production rate and the quenching factor QF given by
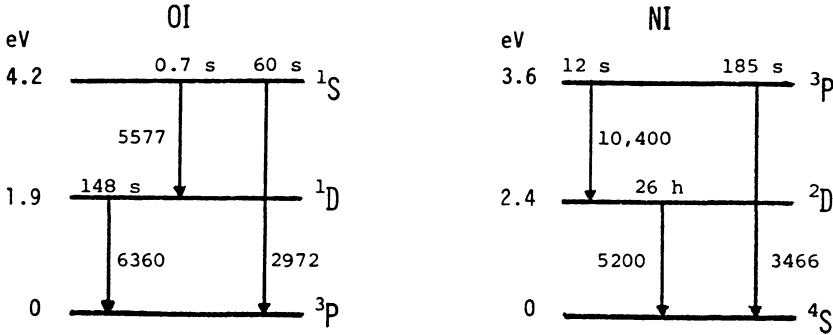
Fig. 1: Low lying states of atomic oxygen and atomic nitrogen
         showing excitation energies, transition wavelengths
         (Å) and term radiative lifetimes.

$$QF = \frac{A_{6360}}{\sum_{^1D} A + \sum k_q n_q}$$

where A is a transition probability, k_q a quenching rate coefficient
for collisions with an atmospheric species of number density n_q. Since
even at 110 km the QFs are 10^{-4} and 10^{-6} for the red oxygen and green
nitrogen doublets, they will not appear in train spectra. However the
upper oxygen state which is depopulated via transitions to the ^1D and
ground states suffers only moderate deactivation at meteoric heights

$$O(^1S) + O(^3P) \rightarrow O(^3P) + O(^3P) \quad k = 5 \times 10^{-11} \exp\left[-\frac{307}{T}\right] \text{ cm}^3\text{s}^{-1}$$

$$O(^1S) + O_2(X^3\Sigma_g^-) \rightarrow O(^3P) + O_2 \quad k = 4 \times 10^{-12} \exp\left[-\frac{871}{T}\right] \text{ cm}^3\text{s}^{-1}$$
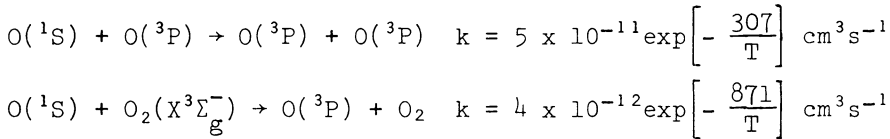
(Slanger and Black 1976; Slanger et al. 1972). The super elastic
collision process

$$O(^1S) + e \rightarrow O(^3P, ^1D) + e \quad k = 0.9 \times 10^{-9} \text{ for } T_e = 200 \text{ K}$$
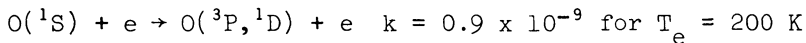
will be important for bright meteors ($\alpha_e \gtrsim 10^{14} \text{ cm}^{-1}$). For $\alpha_e = 10^{14}$
(meteor magnitude approximately zero), the quenching factor, including
the electron deactivation, increases from about 0.05 at 85 km to 0.40
at 110 km. With a probability of $O(^1S)$ production of 0.03 per re-
combination, the emission rate for a zero magnitude meteor is about
2×10^{15} photon s^{-1} cm^{-1} at 110 km; well in excess of that corresponding
to the naked eye threshold. Solution of the diffusion equation set for
the species in an expanding train yields the expected characteristics
of 5577 Å radiation (Baggaley and Cummack 1977). Three characteristics
emerge: a finite rise time for the 5577 Å emission will result from the
two-step mechanism for $O(^1S)$ production; the rise-time will be a well-
defined function of height; a combination of the height profile character-
istic of O^+ deposition and the quenching characteristics implies that
the maximum 5577 Å emission intensity and maximum duration will occur
at about 105 km, 10 km higher than that of the primary meteor light;

emission is expected to be strong only in high velocity meteors
(Baggaley 1975a).
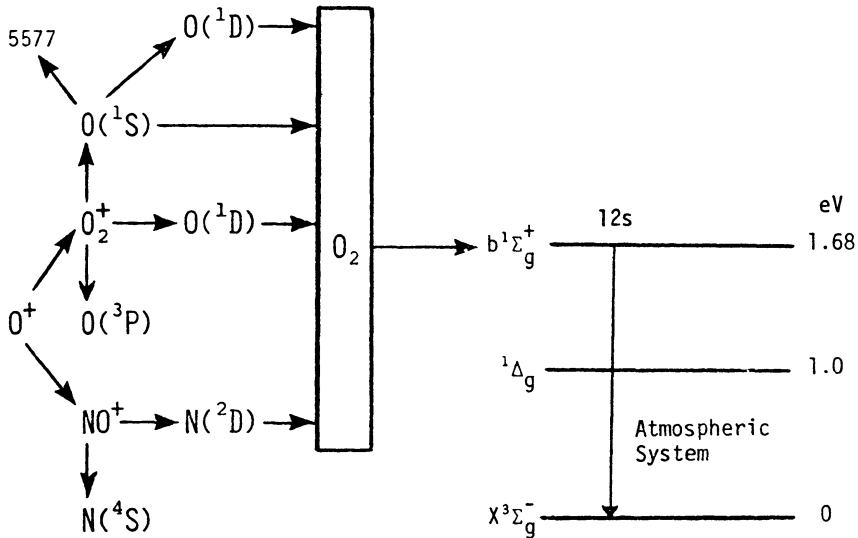
Fig. 2: Possible routes for the loss of atomic oxygen
ionization energy.

A large proportion of the energy not appearing as 5577 Å radiation can
be channelled into excitation of the second electronic state of molecular
oxygen, the upper state of the atmospheric system (Fig. 2). With a
lifetime of 12 s the $^1\Sigma_g^+$ state suffers some deactivation

$$O_2(b^1\Sigma_g^+) + N_2 \rightarrow O_2(X) + N_2 \quad k = 2.2 \times 10^{-15}$$
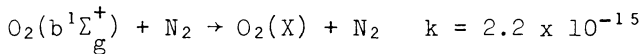
with a quenching factor of 0.4 at 95 km. Since the products of dissoc-
iative recombination will possess translational energy it is possible
that the high vibrational ($v' \gtrsim 5$) levels of the Σ_g^+ state can be excited
yielding a far red emission enduring for a few seconds (Baggaley 1977b).

6.3 Meteoric atoms

Allowed transitions from collisionally excited meteor atoms (M) and
ions are chiefly responsible for meteor primary radiation. Subsequent to
their radiative de-excitation, ground state atoms diffusing into the
ambient atmosphere will have long lifetimes because binary reactions
with O_2 and N_2 do not occur. However slow oxidation is possible by ozone

$$M + O_3 \rightarrow MO + O_2 \quad \Delta H_{oxid} = D_o(MO) - D_o(O_3)$$
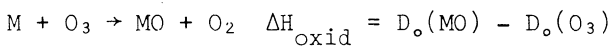
preceeding faster than the formation of dioxide molecules by three body

encounters. In the presence of atomic oxygen metal oxides are reduced

$$MO + O \rightarrow M + O_2 \qquad \Delta H_{red} = D_o(O_2) - D_o(MO)$$
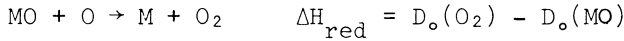
yielding ground state or excited M atoms which subsequently radiate to ground. A metal atom functions as a catalyst, the cycle releasing two oxygen molecules while absorbing an O_3 and an O: the available cycle energy has its origin in photodissociation. Table III lists the values of the reaction energies and the low lying excitation levels of the relevant molecules and atoms associated with the oxidation – reduction cycle.

Table III. Excitation resulting from the oxidation-reduction cycle.

	ΔH_{oxid} eV	molecule transitions			ΔH_{red} eV	lowest level for allowed transition	
		upper state	eV	bands		eV	state
Fe	3.17 ± 0.13	$FeO(^5\Delta)$	2.24	yellow orange	0.87 ± 0.1	2.39	$Fe(^7D)$
Mg	2.39 ± 0.25	$MgO(^1\Sigma^+)$	2.48	green	1.6 ± 0.2	2.70	$Mg(^3P^\circ)$
Si	6.90 ± 0.20	$SiO(^1\pi)$	5.26	U.V.	-3.2	4.91	$Si(^3P)$
Ca	2.87 ± 0.22	$CaO(^1\Sigma)$	1.99	red	1.2 ± 0.02	1.88	$Ca(^3P^\circ)$
Na	1.54 ± 0.20	–	–	–	2.50 ± 0.20	2.09	$Na(^2P)$

Several features are relevant to the production of meteor train luminosity. Ground state meteoric atoms are recycled suffering only slow chemical destruction (lifetime many hours); the photon emission per unit length of expanding meteor column is proportional to the atom line density so that the train emission intensity remains sensibly constant until the column is transversely resolved by the naked eye; the orange-red bands of FeO and CaO are expected and possibly the MgO green band; the only atomic state that can be excited is the ^2P state of sodium. The catalytic cycle

$$Na(^2S) + O_3 \rightarrow NaO(X^2\pi) + O \qquad\qquad k_1$$
$$NaO(X^2\pi) + O \rightarrow Na(^2P) + O_2 \qquad\qquad fk_2$$
$$\rightarrow Na(^2S) + O_2 \qquad\qquad (1-f)k_2$$
$$Na(^2P_{1/2}) \rightarrow Na(^2S_{1/2}) + h\nu(D_1)$$
$$Na(^2P_{3/2}) \rightarrow Na(^2S_{1/2}) + h\nu(D_2)$$
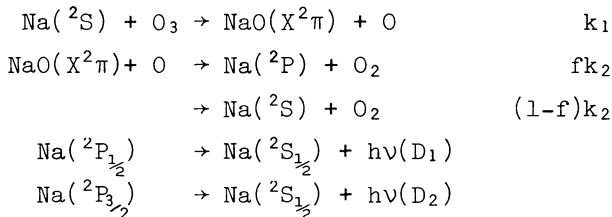
yields emission of the sodium doublet at a rate

$$\varepsilon = \alpha_{Na} f[O_3]k_1 \qquad photon\ cm^{-1}\ s^{-1}$$

with α_{Na} the line density of sodium atoms. Studies of the sodium nightglow luminance

$$B = fk_1 \sum [Na][O_3] \text{photon s}^{-1} \text{ cm}^{-2} (\text{column})^{-1}$$

in association with LIDAR measurements of Na column densities indicate that $0.2 \lesssim f \lesssim 0.6$ (Baggaley 1978b) if $k_1 = 3 \times 10^{-10}$ cm^{3}s^{-1} (Kolb and Elgin 1976). An estimate of α_{Na} can therefore be made for a train emission corresponding to naked eye detection limits. The equivalent meteor magnitude is $\simeq -3$. The depletion of ozone and the effect of train diffusion on enduring train visibility (Baggaley and Cummack 1979b) limit the persistance of visual trains to about one hour.

7. THE FATE OF METEORIC SPECIES

The dispersal of ablation products into the ambient atmosphere proceeds by diffusion and wind shears until eventually the meteor column has lost any identity. The ablation process deposits predominantly neutral species ($\beta \lesssim 0.1$) and ion reactions during column expansion will largely neutralize any meteoric ions, $M^+ \rightarrow M$. Attachment is unlikely to provide a significant sink for meteoric electrons since any electrons can be rapidly recovered from negative atmospheric ions by associative detachment with atomic oxygen.

7.1 Metal species

Diurnal changes in the concentration of minor species in the height region 70-110 km are significant. The lack of night-time O_2 photolysis leads to a large decrease in $[O]$ for heights $\lesssim 85$ km with a corresponding moderate increase in ozone concentrations. Day-time ionization densities increasing from $\sim 10^2$ cm^{-3} at 70 km to $\sim 10^5$ cm^{-3} at 100 km are several orders of magnitude larger than those existing at night. Fig. 3 indicates the pathways available in interactions of metal (M = Fe, Mg, Si, Ca, Ni) species with atmospheric gases while the accompanying table indicates the time-constants associated with the various reactions. Laboratory reaction coefficients depend somewhat on the metal identity (see for example the review of Brown 1973) but the values used here are quite representative. The route $SiO_2^+ \rightarrow SiO^+$ is not possible since the particular reduction reaction with O is endothermic. The photoionization rates ($\sim 5 \times 10^{-7}$s^{-1}) for Fe and Mg correspond to lifetimes of ~ 1 month. Ignoring transport, such a reaction set can be solved to yield the diurnal variation in the concentrations of various species for a particular meteor ablation production function. However the residence time and the relative concentration of each species under equilibrium conditions can be estimated. Above 100 km during daytime charge exchange with ambient ions NO^+ and O_2^+ maintains M^+ which is stable day and night. Even at 95 km the residence time of M^+ against neutralization $\simeq 14$h (day and night) is longer than the ionization time $\simeq 7$h so that above about 90 km M^+ is the dominant species with both neutral and ion oxides negligible. However below ~ 80 km daytime metals will be in atomic form since the M^+ neutralization time is ~ 2h, and M is stable during the night. Near

Ht. km	$M \downarrow MO$	$MO \downarrow M$	$M \downarrow MO_2$	$MO_2 \downarrow MO$	$M \downarrow M^+$	$M^+ \downarrow MO^+$	$MO^+ \downarrow M^+$	$M^+ \downarrow MO_2^+$	$MO_2^+ \downarrow MO^+$	$MO^+ \downarrow M$	$MO_2^+ \downarrow M$
nt 95	1×10^5	1	1.4×10^6	1	5×10^7	50	0.1	5×10^3	0.1	1×10^2	25
dy	1×10^5	1	1.4×10^6	1	5×10^4	50	0.1	5×10^3	0.1	1×10^5	2×10^4
nt 80	2×10^4	20	2.6×10^3	20	10^9	10	2.0	8.6	2.0	2×10^6	5×10^5
dy	5×10^4	5	2.6×10^3	5	10^6	25	0.5	8.6	0.5	2×10^3	5×10^2
nt 70	1×10^3	10^5	1.0×10^2	10^5	2×10^9	0.5	10^4	0.4	10^4	2×10^7	5×10^6
dy	5×10^3	10	1.0×10^2	10	2×10^6	0.5	10	0.4	10	2×10^4	5×10^3

Fig. 3: Reaction scheme for metal species. The table gives the time-constants (seconds) for each route.

70 km iron, magnesium etc. will reside as atoms during the day but will exist largely in the form of neutral oxides at night.

7.2 Alkali metals

Several schemes have considered neutral sodium involving the formation of hydride and dioxide molecules. However it is generally considered that these species are unlikely to play any significant role: rather an equilibrium between oxidation and reduction (Section 6.3) will govern the behaviour of neutral sodium. The ion-oxide reaction scheme that

dominates the life history of Fe^+, Mg^+ etc. is thought to play only a minor role for alkali metals. Laboratory, theoretical and *in situ* mass spectrometer studies show that clustering reactions for Na^+ can be important at mesospheric heights (Richter and Sechrist 1979). It is likely that third order kinetics such as

$$Na^+ + N_2 \rightarrow (Na^+.N_2)\overset{*}{\cdot} + X \rightarrow Na^+.N_2 + X$$
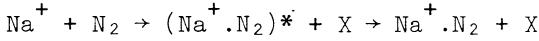
where an excited precursor is stabilized by a third body, dictate the fate of alkali metal species. The reverse process of collisional dissociation and switching reactions in which a loosely bound molecule is replaced can eventually yield large clusters. It is known that water cluster ions formed from O_2^+ and NO^+ are important in D-region chemistry while $Na^+.H_2O$ has been identified in a rocket flight following a meteor shower. For meteoric sodium the sequence (Fig. 4) is initiated by
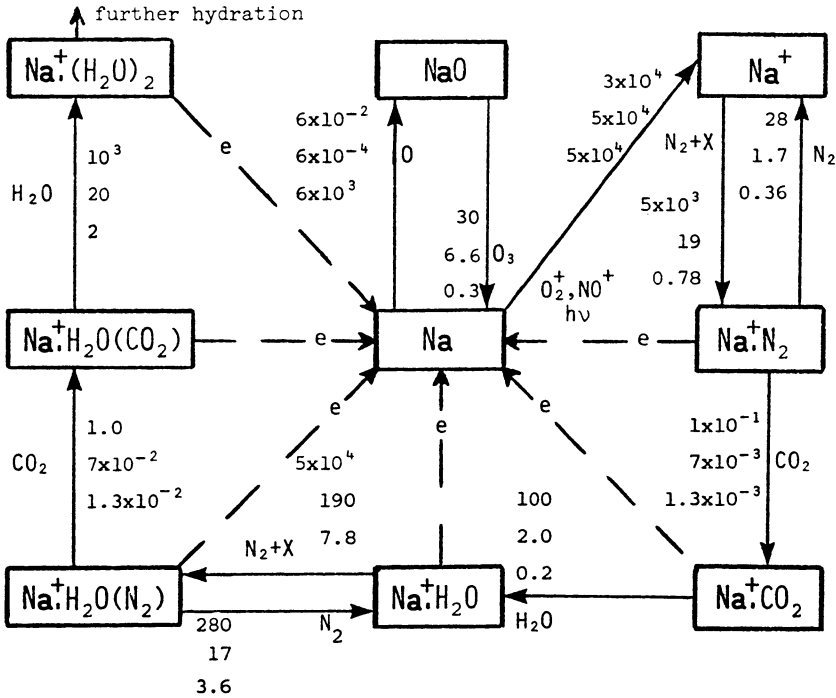
Fig. 4: Sodium reaction scheme. Time-constants (sec.) with coefficients after Richter and Sechrist (1979) are given (in descending order) for heights of 95, 80 and 70 km. Daytime recombination (broken lines) lifetimes are 25, 10^3 and 10^4 s.

three-body clustering with N_2 followed by rapid switching with CO_2 forming $Na^+.CO_2$ which then again switches to form a more stable hydrated ion. Further clustering and switching reactions of hydrated ions produce higher order water complexes.

It is clear that sodium is transferred through the chain rapidly so that even with a high dissociative recombination coefficient ($\sim 10^{-6}$ cm^3 s^{-1}) the lifetime of each ion complex is less than its recombination time with ambient daytime electrons. For heights $\lesssim 95$ km neutralization of clusters will be negligible until the terminal hydrated ion is reached. Those terminal ions below about 80 km not destroyed by thermal dissociation or slow recombination could be a source of aerosols: ions acting as nucleation centres are effective in producing water droplets growth in supersaturated conditions. With low mesopause temperatures ($T \sim 140$ K) ice particles are likely to form, acting under suitable conditions as a source for noctilucent clouds. These large particles would undergo sedimentation into the lower atmosphere; a process providing therefore the ultimate sink.

7.3 Dynamics and models

Since large time-constants are associated with the removal of some particles, long-lived species will be susceptible to dynamical effects operating in the meteor region. Most meteoric atoms are deposited below 105 km (the approximate height of the turbopause) where eddy diffusion operates to establish a state of complete mixing of the atmosphere. The time-scale for turbulent diffusion, H^2/D_e, for the meteor region is about one day for an atmospheric mean scale height $H(\simeq 6$ km). Above the turbopause particles will be redistributed by molecular diffusion, a process much slower than under turbulent conditions ($D_e > 10$ D_M). However, for ions between 90 and 120 km there is the possibility of the operation of a more important transport process. An interaction between east-west winds generated by solar tides and gravity waves and the geomagnetic field tends to concentrate ions at the nodes of the wind profile (a mechanism responsible for the layering of sporadic-E ionization). With a downward wave phase velocity ions are carried to lower heights and coupling maintained until, with an increasingly large ion-neutral particle collision frequency, ions are released to be dispersed by eddy diffusion. The time-scale for ion transport by this process (the corkscrew mechanism, Axford 1967) is a few hours rather than $\gtrsim 1$ day. The evolution of neutral sodium species has been modelled in several studies (for example Megie and Blamont 1977) while a model of sodium ion behaviour has been proposed by Richter and Sechrist(1979). It should be emphasized that uncertainties exist in the models due to a lack of laboratory data; rate coefficients for some reactions are deduced from the corresponding rates for other species.

Twilight resonant scattering from Fe, Ca, Na, K, Ca^+ and others (Mg and Si do not give accessible transitions) has been sought (Gadsden 1969) while a program of LIDAR observation of Na and K has been established by the French group at CNRS (Megie et al. 1978). Enhancements of the

abundances of species following meteor shower occurrence have
been recorded for Na (for example Megie and Blamont 1977), Na.H$_2$O$^+$
(Zbinden et al. 1975) and metallic ions (Herrmann et al. 1978). These and
other studies augmented by laboratory measurements should provide valu-
able data on the important reaction processes and dynamical effects
controlling the behaviour of meteoric primaries and subsequent species
in the atmosphere.

REFERENCES

Axford, W.I. (1967) *Space Research* VII, 126.
Baggaley, W.J. (1977a) *Bull. astron. Inst. Czech.* 28, 277.
Baggaley, W.J. (1977b) *Bull. astron. Inst. Czech.* 28, 356.
Baggaley, W.J. (1978a) *Planet Space Sci.* 26, 979.
Baggaley, W.J. (1978b) *The Observatory* 98, 8.
Baggaley, W.J. (1979a) *Planet. Space Sci.* 27, 905.
Baggaley, W.J. and Cummack, C.H. (1979) *Bull. astron. Instit. Czech.*
     30, 180.
Baggaley, W.J. and Cummack, C.H. (1977) *Can. J. Phys.* 55, 1379.
Baggaley, W.J. and Webb, T.H. (1977) *J atmos. terr. Phys.* 39, 1399.
Brown, N. (1976) *J. atmos. terr. Phys.* 38, 83.
Brown, T.L. (1973) *Chem. Rev.* 73, 645.
CIRA (1972) *Cospar International Reference Atmosphere*, Akademie-Verlag,
     Berlin.
Gadsden, M. (1969) *Annal. Geophys.* 25, 667.
Herrmann, V., Eberhardt P., Hidalgo, M.A., Kopp, E. and Smith, L.G.
     (1978) *Space Research XVIII*, 249.
Hughes, D.W. and Baggaley, W.J. (1972) *Nature* 237, 224.
Kley, D., Lawrence, G.M. and Stone, E.J. (1977) *J. Chem. Phys.* 66,
     4157.
Kolb, C.E. and Elgin, J.B. (1976) *Nature* 263, 488.
Mason, B. (1971) *Handbook of Elemental Abundances in Meteorites*.
     Gordon and Breach, New York.
McKinley, D.W.R. (1956) *J. atmos. terr. Phys.* 8, 76.
McKinley, D.W.R. (1961) *Meteor Science and Engineering*. McGraw-Hill,
     New York pp133.
McIntosh, B.A. and Hadjuk, A. (1977) *Bull. astron. Inst. Czech.*
     28, 280.
Megie, G. and Blamont, J.E. (1977) *Planet Space Sci.* 25, 1093.
Megie, G., Bos, F., Blamont, J.E. and Chanin, M.L. (1978) *Planet.
     Space Sci.* 26, 27.
Moore, C.E. (1972) *A Multiplet Table of Astrophysical Interest*.
     U.S. Dept. of Commerce NSRDS-NBS-40.
Nicholson, T.F. and Poole, L.M.G. (1974) *Planet. Space Sci.* 22, 1669.
Poole, L.M.G. (1978) *Planet Space Sci,* 26, 697.
Poole, L.M.G. (1979) *J. atmos. terr. Phys.* 41, 53.
Richter, E.S. and Sechrist, C.F. (1979) *Geophys. Res. Lett.* 6, 183.
Sharpe, W.E., Rusch, D.W. and Hays, P.B. (1975) *J. Geophys. Res.* 80, 2876.
Sida, D.W. (1969) *Mon. Not. R. astron. Soc.* 143, 37.
Slanger, T.G. and Black, G. (1976) *J. Chem. Phys.* 64, 3764.

Slanger, T.G. Wood, B.J. and Black, G. (1972) *Chem. Phys. Lett.*, <u>17</u>, 401.
Zbinden, P.A. Hidelgo, M.A., Eberhardt, P. and Geiss, J. (1975) *Planet. Space Sci.* <u>23</u>, 1621.

DISCUSSION

Elford: Will electrons in a faint trail at 105-110 km remain hot for a relatively long time?
Baggaley: At about 110 km the electron/ion temperature could be greater than unity for up to 0.1 s so that, for example, underdense echo profiles could be affected.